# Pion scalar form factor and the sigma meson

Torben Hannah*
*Nordita, Blegdamsvej 17, DK-2100 Copenhagen Ø, Denmark*
(Received 9 December 1998; published 26 May 1999)

From recent analysis of the $\pi\pi$ scattering amplitude, it has been claimed that there exists a broad and light $\sigma$ meson. However, if this meson really exists, it must also appear in other observables such as the pion scalar form factor. With the use of unitarity and dispersion relations together with chiral perturbation theory, this form factor is analyzed in the complex energy plane. The result agrees well with the empirical information in the elastic region and reveals a resonance pole at $\sqrt{s}=445-i235$ MeV. This gives further strong evidence for the existence of the $\sigma$ meson. [S0556-2821(99)01113-3]

PACS number(s): 14.40.Cs, 11.30.Rd, 11.55.Fv

It is still controversial whether a broad and light isosinglet scalar meson really exists. After having been omitted from the Particle Data Group for more than twenty years, this scalar meson has reappeared in the last two editions of the Particle Data Group under the entry $f_0(400-1200)$ or $\sigma$ [1]. This reintroduction is based upon several new theoretical analyses [2–4], which have given support to the existence of a broad and light scalar meson. In addition, there has also recently been some experimental indications of $\sigma$ production from central $pp$ collisions [5].

The theoretical evidence for the existence of the $\sigma$ meson comes mainly from model-dependent analysis of $\pi\pi$ scattering [2–4]. However, if this meson in fact exists, it must also appear in other processes containing $\pi\pi$ in the final state. Therefore, in order to further investigate whether the $\sigma$ meson really exists, other processes should also be analyzed. The pion scalar form factor is such a process which can give further important information on the $\sigma$ meson. This is somewhat similar to the well-known case of the $\rho(770)$ meson, where the information on this resonance can be obtained both from $\pi\pi$ scattering and from the pion vector form factor.

The pion scalar form factor has previously been calculated using the inverse amplitude method (IAM) [6,7]. This method is based upon the combination of unitarity and dispersion relations together with chiral perturbation theory (ChPT) [8,9] and has been used in order to extend the range of applicability of ChPT. In particular, the IAM has been applied in order to account for possible resonances since this method, contrary to ChPT, can produce resonance poles in the complex energy plane. In this Brief Report, the scalar form factor is investigated further using the IAM and the result is analyzed in the complex energy plane in order to find possible resonance poles corresponding to the $\sigma$ meson.

The pion scalar form factor $F$ is given by the matrix element of the quark density,

$$\langle \pi^i(p_2)|\bar{u}u+\bar{d}d|\pi^j(p_1)\rangle=\delta^{ij}F(s), \tag{1}$$

where $s=(p_2-p_1)^2$. This form factor is analytical in the complex $s$ plane with a unitarity cut starting at the $\pi\pi$ threshold. In the elastic region the unitarity relation is given by

$$\mathrm{Im}F(s)=\sigma(s)F^*(s)t_0^0(s), \tag{2}$$

where $\sigma(s)$ is the phase-space factor and $t_0^0$ is the isosinglet scalar $\pi\pi$ partial wave. This relation implies that the phase of $F$ will coincide with the $\pi\pi$ phase shift $\delta_0^0$ in accordance with Watson's final-state theorem [10]. The first important inelastic effect starts at around 1 GeV and is due to the $K\bar{K}$ intermediate state. Since the main interest will be in energies well below this inelastic effect, in the following the form factor will only be calculated using the elastic approximation.

The scalar form factor has been calculated to two loops in ChPT both by a dispersive analysis [11] and more recently by a full field theory calculation [12]. The result can be written as

$$F(s)=F^{(0)}(s)+F^{(1)}(s)+F^{(2)}(s), \tag{3}$$

where $F^{(0)}$ is the leading order result, $F^{(1)}$ the one-loop correction, and $F^{(2)}$ the additional two-loop correction. Since the form factor will be normalized to $F(0)=1$ in the following, one has for the leading order term $F^{(0)}=1$. The one-loop correction is given in terms of the single one-loop low-energy constant $l_4^r$ [9], whereas the two-loop correction contains the additional one-loop low-energy constants $l_1^r$, $l_2^r$, and $l_3^r$ together with the two-loop low-energy constants $r_{S2}^r$ and $r_{S3}^r$ [12]. The superscript $r$ indicates that these low-energy constants depend on the renormalization scale $\mu$, whereas the full form factor is scale-independent. Since ChPT is a perturbative expansion, the unitarity relation (2) will only be satisfied perturbatively

$$\begin{aligned}
&\mathrm{Im}F^{(0)}(s)=0,\\
&\mathrm{Im}F^{(1)}(s)=\sigma(s)t_0^{0(0)}(s),\\
&\mathrm{Im}F^{(2)}(s)=\sigma(s)[\mathrm{Re}F^{(1)}(s)t_0^{0(0)}(s)+\mathrm{Re}t_0^{0(1)}(s)].
\end{aligned} \tag{4}$$

This perturbative unitarity will restrict the applicability of ChPT to the very low-energy region. However, with the use

*Electronic address: hannah@nordita.dk

 

of the IAM, the range of applicability of ChPT can be substantially extended to also include resonance regions. The starting point for this method is to write down a dispersion relation for the inverse of the form factor $\Gamma = 1/F$ [6,7]. In this dispersion relation the unitarity relation (2) gives $\mathrm{Im}\Gamma = -\mathrm{Im}F/|F|^2 = -\sigma t/F$. Expanding this quantity to two loops in ChPT gives $\mathrm{Im}\Gamma = -\sigma[t^{(0)}(1-\mathrm{Re}F^{(1)}) + \mathrm{Re}t^{(1)}]$ which can be used on the unitarity cut in the dispersion relation for $\Gamma$. The subtraction constants may also be evaluated by expanding the function $\Gamma$ to two-loop order as $\Gamma^{(2)} = 1 - F^{(1)} + F^{(1)2} - F^{(2)}$. Thus, neglecting possible zeros in the form factor, one has the following dispersion relation:

$$\frac{1}{F(s)} = 1 + a_1 s + a_2 s^2 - \frac{s^3}{\pi}\int_{4M_\pi^2}^{\infty} ds'\,\sigma(s') \times \frac{t_0^{0(0)}(s')[1-\mathrm{Re}F^{(1)}(s')] + \mathrm{Re}t_0^{0(1)}(s')}{s'^3(s'-s-i\epsilon)}, \quad (5)$$

where three subtractions are used in order to make the dispersion integral convergent. This relation can be simplified by writing a dispersion relation for the function $\Gamma^{(2)}$. Using perturbative unitarity (4) one finds this dispersion relation will be exactly similar to the one given in Eq. (5). Thus, the IAM to two loops in the chiral expansion gives the form factor as [6]

$$F(s) = \frac{1}{1 - F^{(1)}(s) + F^{(1)2}(s) - F^{(2)}(s)}. \quad (6)$$

This expression for the form factor is formally equivalent to the [0,2] Padé approximant applied on ChPT and will therefore coincide with the chiral expansion up to two-loop order. However, with the IAM the range of applicability of ChPT is substantially extended. This is based upon the fact that the expansion of $t/F$ used in the IAM works rather well over a much larger region than the corresponding expansion of $F^*t$ used in ChPT. In fact, the former expansion works well throughout the elastic region, even when the form factor has a resonant character [7].

However, the IAM may generate poles on the physical sheet which violate the analyticity requirement. These poles are caused by the high-energy part of the dispersion integral in Eq. (5). Since this part is not expected to be well approximated, it may cause the right-hand side of Eq. (5) to vanish and thereby generate spurious poles in the form factor. These poles should in principle be removed without any significant influence in the region of applicability of the IAM. A rather general method to remove possible poles and thereby restore analyticity is to put the imaginary part of the IAM back into a dispersion relation. With three subtractions the result can be written as

$$F(s) = 1 + \tfrac{1}{6}\langle r^2\rangle s + cs^2 + \frac{s^3}{\pi}\int_{4M_\pi^2}^{\infty} \frac{\mathrm{Im}F(s')ds'}{s'^3(s'-s-i\epsilon)}, \quad (7)$$

where both the subtraction constants and Im$F$ are calculated from the IAM (6). Here, it is assumed that Im$F$ does not contain any poles on the unitarity cut and three subtractions are used in order to suppress the high-energy part of the dispersion integral. Without any poles Eq. (7) is just an identity, but with poles the output will in general be different from the input. However, in the region where the IAM is applicable, the difference between the form (7) and the form (6) should be small. In fact, this method to remove possible poles is equivalent to the subtraction of the poles on the physical sheet from the original IAM (6). This will be discussed in more detail elsewhere [13].

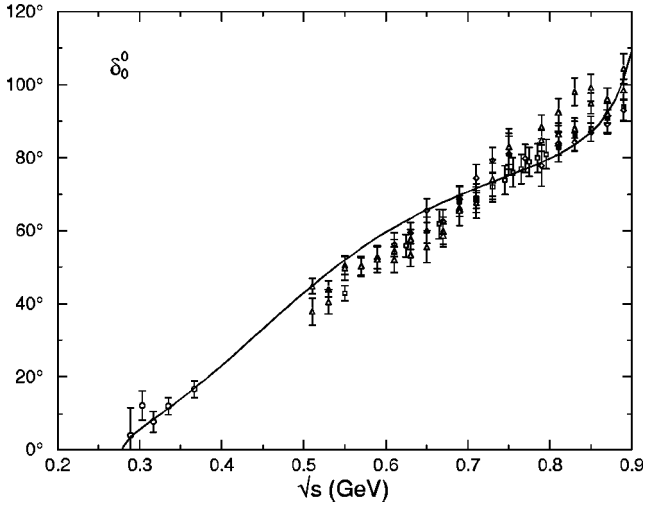


FIG. 1. The phase $\delta_0^0$ of the scalar form factor in the elastic region below $\sqrt{s} = 0.9$ GeV. The experimental $\pi\pi$ phase shifts are from Ref. [14] (circles), Ref. [15] (squares), Ref. [16] (diamonds), and Ref. [17] (triangles).

The IAM to two loops depends on a number of low-energy constants which have to be determined phenomenologically. Unfortunately, the scalar form factor is not directly accessible to experiment. However, in the elastic region the phase of $F$ is given by the $\pi\pi$ $I=0$ $S$ phase shift $\delta_0^0$, which is known experimentally. Fitting these phase shifts up to 0.9 GeV [14–17] and using the value of the pion scalar radius $\langle r^2\rangle = 0.60$ fm$^2$ [11,18], some of the low-energy constants in the IAM to two loops have previously been determined without taking possible poles into account [6]. Here, in order to remove spurious poles, this fit is repeated with the form factor given by Eq. (7). The result is shown in Fig. 1 together with the experimental $\pi\pi$ phase shifts, from where it is observed that the IAM agrees rather well with the main bulk of the data all the way up to 0.9 GeV. Thus, the IAM satisfies Watson's final-state theorem [10] quite well in the whole elastic region. This fit gives the following values for the low-energy constants:

$$l_4^r = 1.53\times 10^{-3},$$
$$r_{S2}^r = 2.25\times 10^{-3}, \quad (8)$$
$$r_{S3}^r = 7.60\times 10^{-5}$$

at the renormalization scale $\mu = M_\rho = 770$ MeV. Since the experimental data are not very consistent with each other,

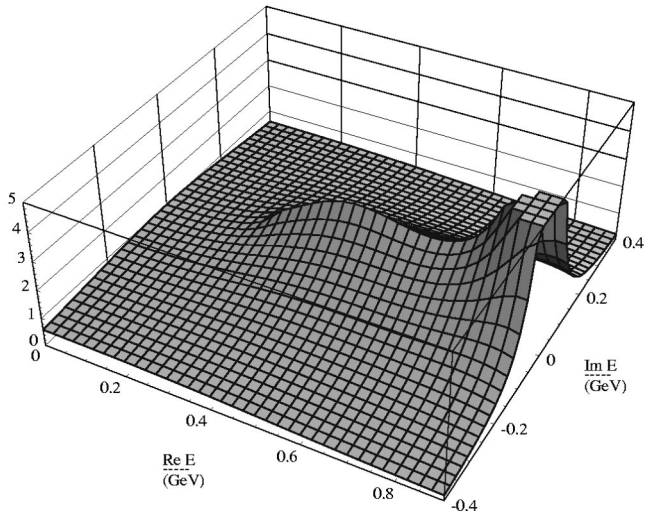


FIG. 2. The scalar form factor $|F|^2$ in the complex energy plane on the first Riemann sheet. The complex energy $E$ is defined according to $s=(\mathrm{Re}E+i\,\mathrm{Im}E)^2$.

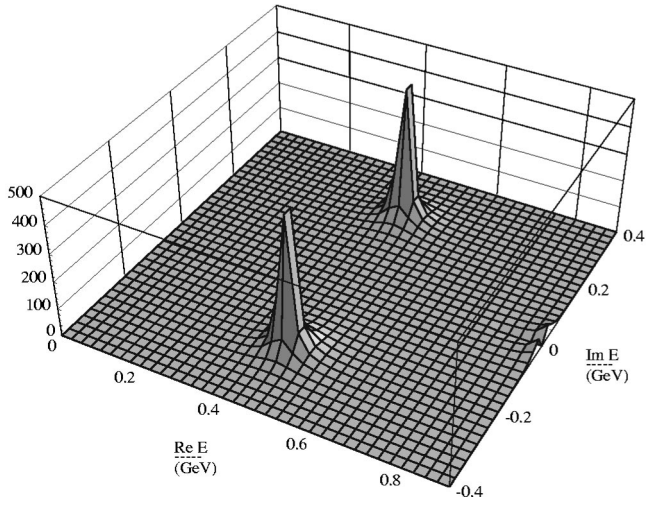


FIG. 3. The scalar form factor $|F|^2$ in the complex energy plane on the second Riemann sheet.

there has not been assigned any error bars on these low-energy constants. However, the obtained values of $l_4^r$ and $r_{S3}^r$ agree rather well with the recent determination of these low-energy constants using two-loop ChPT [12]. As for $r_{S2}^r$, this low-energy constant has so far only been estimated on the basis of the resonance saturation hypothesis [19] with a result [12] that is somewhat smaller than the value obtained above. In the future, it might be possible to determine this two-loop low-energy constant from independent observables [20] and thereby check the value obtained here.

The scalar form factor can be defined in the whole complex $s$ plane. Since it contains cuts starting at the $\pi\pi$ threshold, this will involve different Riemann sheets. In the elastic approximation there are two Riemann sheets, which are defined according to the sign of the center of mass momenta $q=\sqrt{s-4M_\pi^2}/2$. The first or physical sheet has positive values of $\mathrm{Im}q$, whereas the second or unphysical sheet has negative values of $\mathrm{Im}q$. The form factor given by either Eq. (6) or Eq. (7) can indeed be extended analytically to the whole complex $s$ plane. This analytic continuation will involve infinitely many Riemann sheets since the cut in the IAM comes from logarithmic functions. However, only two of these sheets correspond to the first and second Riemann sheet that the form factor should reproduce.

In Fig. 2 the absolute square of the form factor (7) is shown in the complex energy plane on the first Riemann sheet. On the real axis the result agrees very well with the result of a dispersive analysis [11,18], where the scalar form factor has been determined in terms of the experimental $\pi\pi/K\bar{K}$ phase shifts. Furthermore, the form factor (7) is analytic in the whole complex energy plane with the correct cut structure starting at the $\pi\pi$ threshold. This is different from the original IAM (6) which generates a pole on the negative $s$ axis. However, this pole is removed by using the form (7) without any significant influence on the result in the region shown in Fig. 2.

From this figure it is also observed that around 0.4 $-0.5$ GeV the form of $|F|^2$ is somewhat reminiscent of a resonant structure. However, in order to investigate whether this form is really associated with a resonance, one has to consider the second Riemann sheet. On this sheet resonances are characterized by poles in the complex energy plane, where the mass $(M_R)$ and width $(\Gamma_R)$ of the resonance can be related to the position of the pole by

$$\sqrt{s_{pole}}=M_R-i\frac{\Gamma_R}{2}. \tag{9}$$

In Fig. 3 the absolute square of the form factor (7) is shown in the complex energy plane on the second Riemann sheet. One finds that $|F|^2$ indeed generates two complex conjugated poles corresponding to a broad and light resonance. In fact, the position of these poles is the same for the two expressions of the form factor given by Eq. (6) and Eq. (7), respectively. From the position of the pole, the mass and width of this $\sigma$ meson is given by

$$M_\sigma=445\ \ \mathrm{MeV}, \quad \Gamma_\sigma=470\ \ \mathrm{MeV}. \tag{10}$$

This compares rather well with the values $M_\sigma=470$ MeV and $\Gamma_\sigma=500$ MeV obtained in Ref. [2]. However, rather different values for $M_\sigma$ and $\Gamma_\sigma$ have also been obtained with other theoretical models [3,4]. Therefore, it is important to reduce the model dependence when the mass and width of the $\sigma$ meson are determined. The IAM is based solely on the use of unitarity and dispersion relations together with ChPT. Therefore, within this approach, any model dependence in the mass and width of the $\sigma$ meson is due to higher order terms in the chiral expansion together with the present uncertainties in the values of the low-energy constants.

The IAM is in fact a systematic approach which can be applied to any given order in the chiral expansion. Originally, this method was applied to the scalar form factor in the one-loop approximation [7] with a result that is formally equivalent to the [0,1] Padé approximant applied on ChPT. In this case the IAM depends on the single one-loop low-energy constant $l_4^r$ which can be determined from the ratio

$F_K/F_\pi$ [9,20]. With this low-energy constants fixed, the IAM to one loop agrees rather well with the empirical information up to about 0.5 GeV. The one-loop approximation also contains a pole on the negative $s$ axis. However, this pole can be removed by using the method discussed previously without any significant influence on the result in the elastic region. Extending this result to the whole complex energy plane, one finds that the IAM to one loop also generates a resonance pole, where the corresponding mass and width of this resonance are given by

$$M_\sigma = 463 \text{ MeV}, \quad \Gamma_\sigma = 393 \text{ MeV}. \tag{11}$$

Comparing these values with the values obtained from the IAM to two loops (10), it is observed that the masses are very similar, whereas the difference in the widths is somewhat larger. However, this difference is not significant compared to the large uncertainty in the width of the $\sigma$ meson given by the Particle Data Group [1]. In view of this the convergence of the IAM is satisfactory for both the mass and width of the $\sigma$ meson. Hence, the corrections to the values given in Eq. (10) due to even higher orders in the chiral expansion are expected to be of little importance. There is also an uncertainty in the obtained values for $M_\sigma$ and $\Gamma_\sigma$ coming from the uncertainties in the values of the low-energy constants. However, this effect should also be rather small and could be estimated when the values of the low-energy constants in the IAM are determined more accurately.

The IAM is not restricted to the scalar form factor but this method is in fact quite general and has been applied to other processes as well. In particular, the IAM has been applied to $\pi\pi$ scattering where it also generates a resonance pole corresponding to the $\sigma$ meson [21]. In fact, the mass and width of the $\sigma$ resonance obtained from $\pi\pi$ scattering, $M_\sigma = 440$ MeV and $\Gamma_\sigma = 490$ MeV, agree very well with the values obtained in Eq. (10). This strongly supports the consistency of the IAM and gives additional evidence for the existence of the $\sigma$ meson.

To summarize, the pion scalar form factor has been calculated by the use of unitarity and dispersion relations together with the chiral expansion. In order to satisfy the analyticity requirement, possible poles on the physical sheet are removed from this IAM. The result agrees well with both the experimental $\pi\pi$ phase shifts and a dispersive analysis in the whole elastic region. Making an analytic continuation of the scalar form factor to the complex energy plane, one finds a resonance pole corresponding to a broad and light scalar meson. The values for the mass and width of this $\sigma$ meson are obtained in a rather model independent way, contrary to previous determinations where different theoretical models were applied. Indeed, any model dependence in the obtained values for $M_\sigma$ and $\Gamma_\sigma$ should be rather small compared to the present uncertainty in these quantities. All this gives further strong evidence for the existence of the controversial broad and light $\sigma$ meson.


[1] Particle Data Group, C. Caso *et al.*, Eur. Phys. J. C **3**, 1 (1998); Particle Data Group, R. M. Barnett *et al.*, Phys. Rev. D **54**, 1 (1996).

[2] N. A. Törnqvist and M. Roos, Phys. Rev. Lett. **76**, 1575 (1996).

[3] S. Ishida *et al.*, Prog. Theor. Phys. **98**, 1005 (1997); S. Ishida *et al.*, *ibid.* **95**, 745 (1996).

[4] R. Kamiński, L. Leśniak, and B. Loiseau, Phys. Lett. B **413**, 130 (1997); R. Kamiński, L. Leśniak, and J.-P. Maillet, Phys. Rev. D **50**, 3145 (1994).

[5] GAMS Collaboration, D. Alde *et al.*, Phys. Lett. B **397**, 350 (1997).

[6] T. Hannah, Phys. Rev. D **55**, 5613 (1997).

[7] T. N. Truong, Phys. Rev. Lett. **61**, 2526 (1988).

[8] S. Weinberg, Physica A **96**, 327 (1979).

[9] J. Gasser and H. Leutwyler, Ann. Phys. (N.Y.) **158**, 142 (1984); Nucl. Phys. **B250**, 465 (1985).

[10] K. M. Watson, Phys. Rev. **95**, 228 (1954).

[11] J. Gasser and U. G. Meissner, Nucl. Phys. **B357**, 90 (1991).

[12] J. Bijnens, G. Colangelo, and P. Talavera, J. High Energy Phys. **5**, 14 (1998).

[13] T. Hannah and T. N. Truong (in preparation).

[14] L. Rosselet *et al.*, Phys. Rev. D **15**, 574 (1977).

[15] S. D. Protopopescu *et al.*, Phys. Rev. D **7**, 1279 (1973).

[16] B. Hyams *et al.*, Nucl. Phys. **B64**, 134 (1973); W. Ochs, Ph.D. thesis, Ludwig-Maximilians-Universität, 1973.

[17] P. Estabrooks and A. D. Martin, Nucl. Phys. **B79**, 301 (1974).

[18] J. F. Donoghue, J. Gasser, and H. Leutwyler, Nucl. Phys. **B343**, 341 (1990).

[19] G. Ecker *et al.*, Nucl. Phys. **B321**, 311 (1989).

[20] T. Hannah, Phys. Rev. D **54**, 4648 (1996); J. Gasser and H. Leutwyler, Nucl. Phys. **B250**, 517 (1985).

[21] A. Dobado and J. R. Peláez, Phys. Rev. D **56**, 3057 (1997).